Residual interactions in unfolded bile acid-binding protein by ^{19}F NMR

H. Kenney Basehore and Ira J. Ropson*

Department of Biochemistry and Molecular Biology, Penn State University College of Medicine, Hershey, Pennsylvania

Received 1 July 2010; Revised 7 November 2010; Accepted 8 November 2010
DOI: 10.1002/pro.563
Published online 29 November 2010 proteinscience.org

Abstract: The folding initiation mechanism of human bile acid-binding protein (BABP) has been examined by ^{19}F NMR. Equilibrium unfolding studies of BABP labeled with fluorine at all eight of its phenylalanine residues showed that at least two sites experience changes in solvent exposure at high denaturant concentrations. Peak assignments were made by site-specific 4FPhe incorporation. The resonances for proteins specifically labeled at Phe17, Phe47, and Phe63 showed changes in chemical shift at denaturant concentrations at which the remaining five phenylalanine residues appear to be fully solvent-exposed. Phe17 is a helical residue that was not expected to participate in a folding initiation site. Phe47 and Phe63 form part of a hydrophobic core region that may be conserved as a site for folding initiation in the intracellular lipid-binding protein family.

Keywords: protein folding; bile acid-binding protein; fluorine NMR; hydrophobic collapse; intestinal fatty acid-binding protein; residual structure; unfolded proteins

Introduction

All of the information required for a protein to fold to the native structure is found in the amino acid sequence, but the mechanism by which folding occurs is still unclear. One aspect of this problem can be examined by studying the folding of proteins that share a common native structure but have different amino acid sequences. The intracellular lipid-binding protein (iLBP) family is a group of 14–16 kDa proteins that share a common structure, consisting of 10 antiparallel β-strands that form two nearly orthogonal β-sheets surrounding an internal ligand-binding cavity that is gated by two short α-helices (Fig. 1). The amino acid sequences in iLBP's have as little as 15% sequence identity between family members,[1,2] in spite of their highly conserved tertiary structure.

Several folding studies have addressed this question in the iLBP family.[2–6] Kinetic analysis of the folding mechanism of two family members, intestinal fatty acid-binding protein (IFABP) and bile acid-binding protein (BABP, also ileal lipid-binding protein, or ILBP) identified an intermediate state early in IFABP folding that was not observed for wild-type BABP,[2,7] probably due to a decrease in the number and hydrophobicity of residues in the hydrophobic core region of BABP. Single site mutations that altered the BABP hydrophobic core region to more resemble that of IFABP resulted in a folding mechanism similar to IFABP, supporting specific hydrophobic collapse as an initiating event in the folding reaction in these proteins.[4] This mechanism had been proposed earlier,[7] and evidence from several other studies of IFABP provided support for a folding initiation site in this region,[8,9] yet an early intermediate state in this region has not been observed for WT-BABP. It is possible, however, that the intermediate state is present, but

Abbreviations: BABP, bile acid-binding protein; DHFR, dihydrofolate reductase; 4FPhe, 4-fluoro phenylalanine; 6FTyr, 6-fluoro tyrosine; iLBP, intracellular lipid-binding protein; IFABP, intestinal fatty acid-binding protein; IPTG, isopropyl β-D thiogalactopyranoside; ppm, parts per million; Phe, phenylalanine; Tyr, tyrosine.

Additional Supporting Information may be found in the online version of this article.

Heather Basehore's current address is Research Service, Department of Veterans Affairs Medical Center, Coatesville, PA 19320.

Grant sponsor: NIH; Grant numbers: GM-57906, RR021172; Grant sponsor: The Pennsylvania Department of Health Tobacco Settlement Funds.

*Correspondence to: Ira J. Ropson, Ph.D., Penn State College of Medicine, Department of Biochemistry and Molecular Biology, 500 University Drive H171, Hershey, PA 17022.
E-mail: iropson@psu.edu

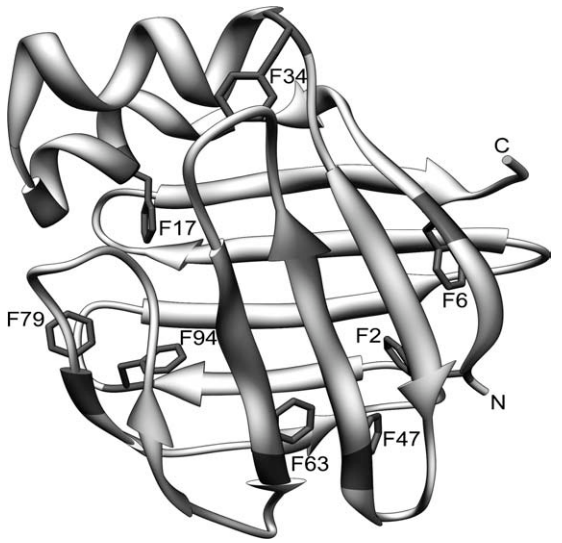

Figure 1. Structure of human BABP (PDB: 1o1u).

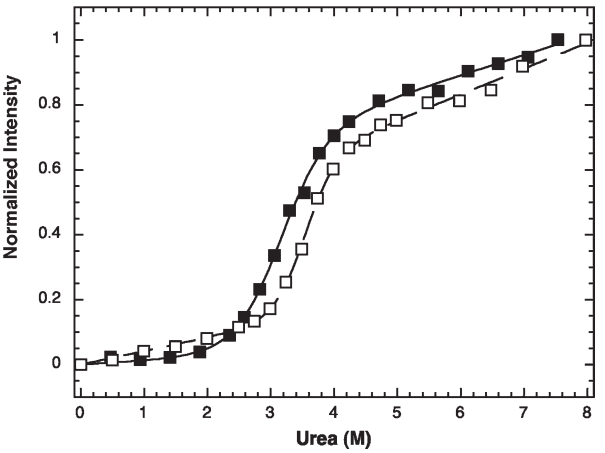

Figure 2. Equilibrium fluorescence unfolding of WT-BABP (open squares) and 4Fphe-BABP (closed squares). The lines are the fit to a two state model of the equilibrium unfolding of WT-BABP and 4Fphe-BABP.

does not accumulate to a high enough population to be detected by optical methods. ^{19}F NMR has been shown to be very sensitive to the presence of sparsely populated conformations at equilibrium in the iLBPs,[7,10,11] and was used to determine whether BABP initiates folding via a mechanism of hydrophobic collapse of specific core residues.

Results

Equilibrium unfolding of BABP

Wild-type BABP has been shown to fold via a two-state mechanism with no significant accumulation of intermediates at equilibrium.[6] Addition of a histidine tag and the 4FPhe label did not perturb the two-state mechanism, suggesting that no significant concentration of an intermediate state exists for any of the variants at equilibrium. Uniform incorporation of 4FPhe perturbed the equilibrium folding compared with unlabeled BABP, with decreases in ΔG_{H2O} (the extrapolated stability of the protein to 0*M* denaturant), m_G (the dependence of ΔG on denaturant concentration), and in the midpoint for urea denaturation (Fig. 2). A similar smaller destabilization was noted (Table 1) with incorporation of 6FTrp in rat-BABP.[6] This result contrasts to previous studies of the folding of other fluorine-labeled proteins in the iLBP family,[6,7,12] where a slight stabilization of the protein upon incorporation of fluorine-labeled amino acids was typically observed. This stabilization was thought to be due to the increased hydrophobicity of fluorinated aromatic amino acids compared with their unlabeled counterparts,[6] and it is not clear why BABP does not show this behavior.

Table I. *Equilibrium Unfolding Data*

Protein	Midpoint (M)	ΔG_{H2O} (kcal mol^{-1})	m_G (kcal mol^{-1} M^{-1})
BABP(6His)	3.53 ± 0.02	7.81 ± 0.61	−2.21 ± 0.17
4FPhe-BABP (6His)	3.14 ± 0.03	4.66 ± 0.34	−1.49 ± 0.11

NMR of site-specific 4FPhe incorporation

Equilibrium unfolding studies suggest that BABP is unfolded at urea concentrations higher than 4*M*. However, examination of the NMR spectra of 4FPhe-BABP between 4 and 8*M* urea reveals that at least two amino acids continue to have resonance changes as denaturant increases (Fig. 3). To identify the regions

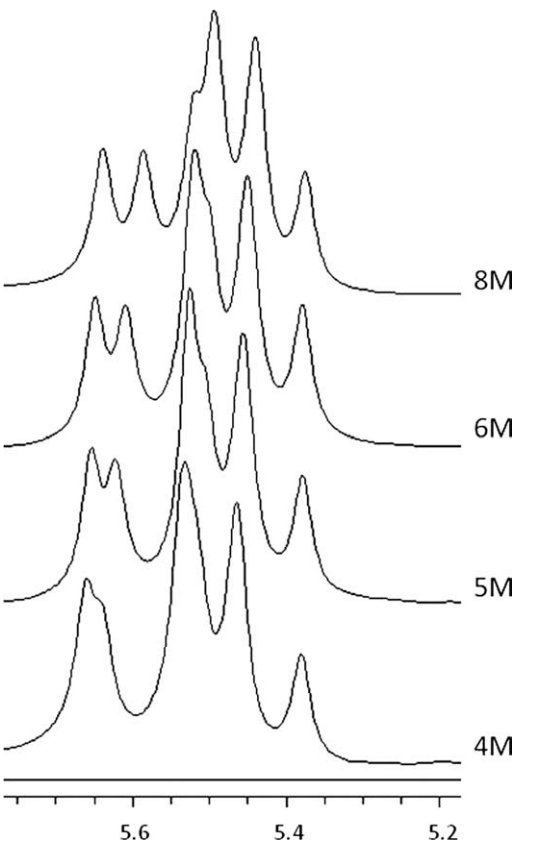

Figure 3. ^{19}F NMR spectra of native 4FPhe-BABP. The chemical shift is from 6FTrp.

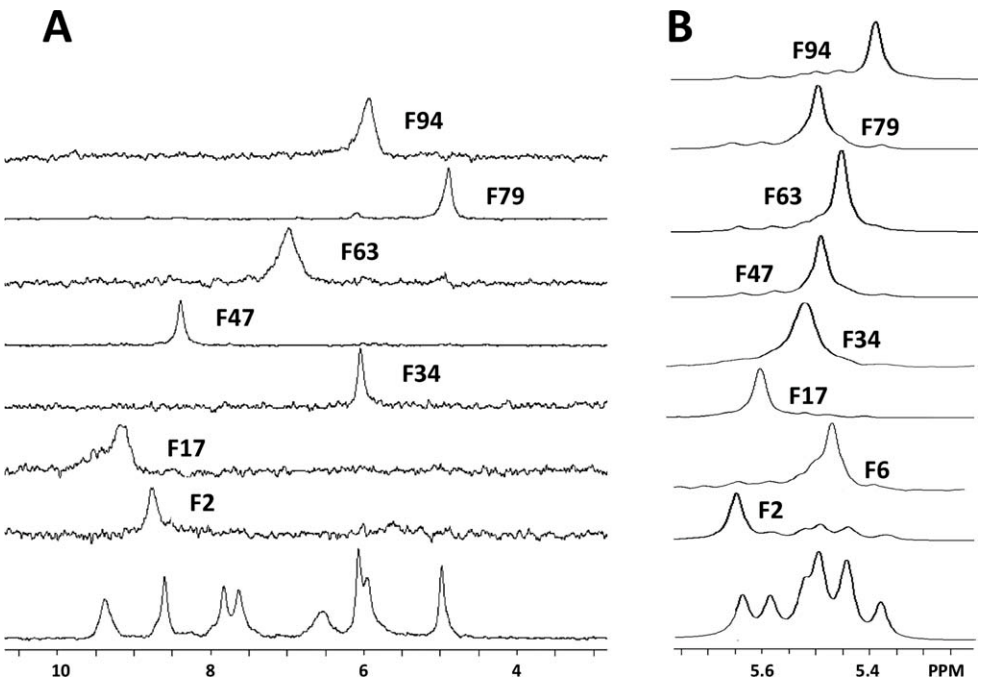

Figure 4. Native state (A) and unfolded (B) resonance spectra for variants labeled site specifically at Phe residues, aligned with the 4Phe-BABP spectrum. The chemical shift is from 6FTrp. Because of poor expression, no native spectra is shown for the Phe6 mutant. Note the differences in scale between Figure A and B, owing to the much smaller differences in chemical shift of unfolded peaks compared with native.

of BABP involved, the NMR peaks were assigned by site-specifically incorporating fluorine at each Phe residue in the sequence. Single-site incorporation of 4FPhe typically resulted in yields of ~10–20 mg of protein per liter of media. The single-site labeled proteins showed one major ^{19}F NMR peak, with weak background labeling of the remaining Phe residues. This is the "contamination" described in the original publication[13] and was useful in the assignment of the peaks in the fully labeled spectra.[10] Fluorine-NMR spectra were collected for each of the single-site variants, and the resulting spectra aligned reasonably well with the spectra observed for the protein labeled with fluorine at all eight Phe sites (Fig. 4). Phe47 and Phe63 appear to be slightly deshielded in the single site preparation compared with the protein labeled with fluorine at all eight sites, because the single-labeled peaks are shifted downfield from the corresponding peaks in the fully labeled protein. The fluorine nucleus is exceptionally sensitive to its local environment, and these two residues are in close proximity to each other in the native state (Fig. 1). As such, the additional shielding provided by the two fluorine nuclei in close proximity is likely to change their chemical shift, as shown in studies of uniformly and site-specifically labeled IFABP.[14] Similarly, it is likely that the Phe2 peak is also shifted in the single-site labeled protein compared with the wild-type, because of the close proximity of the Phe2 aromatic ring to that of Phe47. Further experiments would be required to check the assignments of the native state resonances of the 4FPhe-BABP spectrum but are not necessary for interpretation of the results presented here.

The response of the NMR spectra to increasing denaturant was monitored for each of the single-site 4FPhe labeled proteins (Fig. 5). The response of chemical shift to denaturant was not uniform among the eight residues. NMR peaks that continue to change at high denaturant concentrations represent residues that might be involved in an early folding intermediate. Chemical shifts for each of the single-site 4FPhe-labeled proteins are plotted against urea concentration (Fig. 6). There is a linear relationship between chemical shift and urea concentration over this denaturant range for each resonance. Lower values for slope indicate that the resonance shows little dependence on denaturant concentration. Higher slope values indicate greater changes in environment for that residue at higher denaturant concentrations. All peaks do not have the same degree of chemical shift behavior, which indicates that different residues experience different environments under solution conditions where the protein is completely unfolded by fluorescence or CD criteria. As a control, the ^{19}F NMR spectra of free 4FPhe in solution were collected, and the chemical shift showed a linear relationship to urea concentration. The slope of the best-fit line for the 4FPhe reference was 0.0002 ppm/M, indicating almost no change in chemical shift over the range of 4 to 8*M* urea, excluding instrumental artifacts as the cause of the chemical shift behavior of a few of the BABP residues.

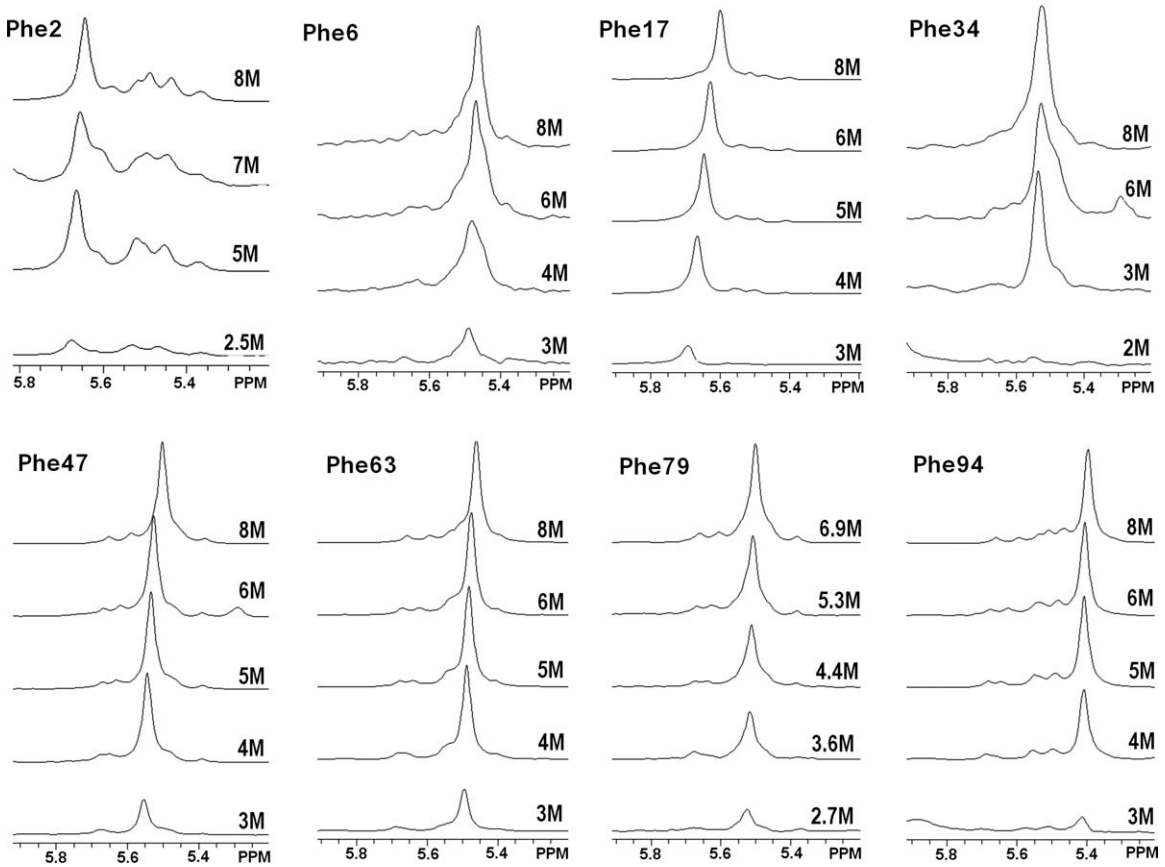

Figure 5. ^{19}F NMR unfolding spectra of BABP site specifically labeled at each of the eight Phe residues. The resonances for Phe17, Phe47, and Phe63 continue to change as denaturant concentration increases, whereas the resonances for the remaining five Phe residues are nearly constant in response to increasing denaturant. Contamination of ^{19}F-label incorporating at sites not selected in the given experiment can be seen for some of the spectra (e.g., Phe2-BABP). Peak shifts for all proteins are shown in ppm from the 6FTrp reference peak. All peaks were normalized for intensity compared with the known concentration of the reference standard. Apparent differences in intensity at lower denaturant concentrations are due to the remaining intensity at the native state chemical shift, which is out of range of the scale shown.

Phe2, Phe6, Phe34, Phe79, and Phe94

Examination of the single-site incorporation NMR data showed that five of the Phe residues have minimal changes in chemical shift between 4 and 8*M* urea (Fig. 6). Phe34 had the lowest dependence of chemical shift on denaturant concentration. Phe6 and Phe94 had a slightly higher dependence of chemical shift on denaturant concentration than Phe35, and Phe79 and Phe2 were slightly higher still. The integrated peak intensity for Phe79 appeared to increase moderately in peak area with increasing denaturant concentration (Fig. 5), which might indicate the presence of another conformation in chemical exchange; however, line width analysis reveals that the peaks are not broadened at the lower urea concentrations, and no other peak was observed in these spectra, suggesting that chemical exchange on either the intermediate or slow exchange time scales is unlikely. Further, analysis of the total integrated peak intensity for the protein labeled with ^{19}F at all Phe sites for the combined eight resonances did not change over this range, which does not support an alternative protein conformation at this site. Based on the chemical shift behaviors, these five Phe residues appear to unfold uniformly and experience about the same degree of solvent exposure to urea, indicating that they are not likely to be involved in any region of residual structure in the unfolded state of BABP. The three remaining Phe residues have chemical shift behaviors that continue to change at a significantly higher rate in response to higher denaturant concentrations.

Phe17

The Phe17 resonance shifted more than any other residue in response to denaturant concentration. Phe17 is located within the first α-helix of BABP. Experiments published on variants of IFABP in which the helical region has been removed revealed that the helices in IFABP have little effect on the rate of formation or overall stability of the β-barrel structure.[15,16] Because of the structural similarities between the wild-type and helix-less IFABP proteins, the helices were suggested to play little if any role in the stability of the protein or in the mechanism of the β-barrel folding. Thus, Phe17 was not

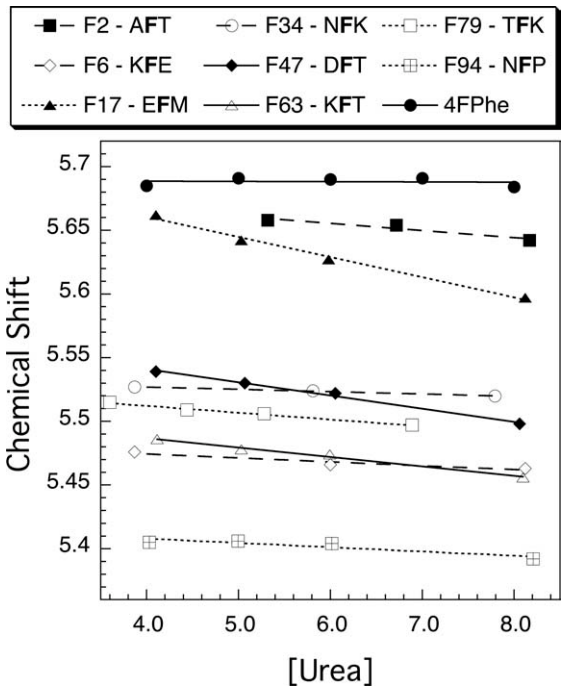

Figure 6. Plot of NMR resonance peak shift versus urea concentration. Each of the lines corresponds to a linear fit for the dependence of chemical shift for each 4FPhe-labeled residue in BABP on denaturant concentration. The legend shows the local amino acid sequence around each 4FPhe. The dependence of the 4FPhe standard on denaturant concentration was shifted by −0.3 ppm for clarity.

expected to show any residual structure in unfolded BABP. However, a recent study of a helix-less mutation in BABP showed that the helices influence the stability of BABP much more dramatically than IFABP, with the helix-less BABP unfolded under physiological conditions.[17] Addition of ligand to the helix-less protein resulted in recovery of the structure, but the apo-protein conformation had NMR and CD properties similar to that of a disordered protein. The helical region in BABP may play a more significant role in the stability and possibly in the folding of this protein.[17] The behavior of Phe17 upon unfolding presented here supports this suggestion. However, if it were the case that Phe17 were involved in an early folding intermediate, it is likely that other nearby aromatic residues would show similar behavior. Phe34 is in the second ß-strand, in close proximity to the end of helix 2, but appears to show no unusual dependence of chemical shift at high urea concentrations. Preliminary experiments with 4FTyr BABP indicate that one of the four Tyr resonances has a much steeper dependence of resonance frequency on denaturant than the other three residues, suggesting that residual structure is present at that site (not shown), but the Tyr resonances have not been assigned. One of the four Tyr residues (Tyr14) is at the start of helix 1, in close proximity to Phe17 and may be responsible for this behavior. Of all aromatic residues in BABP, only Phe17 and Tyr14 are in a helix. A study in another member of the iLBP family, cellular retinoic acid binding protein I, showed that a short peptide corresponding to this region forms helical structure in solution.[18] Predictive modeling using the Agadir program suggests that the helix sequence in BABP has a similar propensity to form helical secondary structure,[19] but the structure is not expected to persist at high urea concentrations. The role of Phe17 and of the α-helical region in BABP folding remains unclear.

Phe47 and Phe63

Phe47 in BABP is homologous to Phe47 in IFABP, which was originally proposed to be involved in folding initiation;[7] more recent evidence suggested that it may not be appropriate to include this residue in the folding initiation site.[10] Phe63 in BABP is a homolog for Phe62 in IFABP, which also has been suggested to participate in the early folding intermediate in IFABP.[7,14] The chemical shift changes between 4 and 8*M* urea in the BABP experiments are greater for Phe63 and Phe47 than for any Phe except for Phe17. This could be explained by residual structure persisting in this region at denaturant concentrations for which the majority of the structure has become unfolded. The two residues are in close contact in the native protein, so any structure that they both participate in could have native-like characteristics. Evidence of their interaction is seen in the native state spectra, in which the NMR peaks for single-site labeled protein are significantly deshielded in comparison with the corresponding peaks in the individual 4FPhe-BABP spectra. The deshielding is a consequence of the close proximity of the two fluorine groups in the fully labeled protein being eliminated in the single-site labeled proteins. Interaction between these two residues is conserved across all members of the iLBP family.[5] This interaction may play a role in initiation of protein folding and may represent an evolutionarily conserved folding mechanism.

Discussion

Local electrostatic field and noncovalent interactions with nearby atoms cause chemical shift differences for fluorine-labeled residues in protein spectra. The fluorine environment in a labeled protein changes significantly from the native to the denatured state, with the major influences on fluorine shielding coming both from changes in intermolecular interactions with the changing solvent environment and alterations in the interactions with other protein atoms upon unfolding.[20,21] As solvent exposure is not expected to differ for a ^{19}F on a phenylalanine that is fully solvent-exposed, the changes in chemical shift observed at high urea concentrations are due either to the electrostatic environment of the local primary structure or to longer range intramolecular interactions. Close inspection of the local sequences surrounding each Phe

residue for polarity and charge does not reveal an obvious relationship between the local sequence and the chemical shift behavior (Fig. 6 legend). Therefore, we propose that the chemical shift changes at high denaturant concentrations may be due to residual long-range intramolecular interactions.

The data presented here for BABP do not indicate the presence of multiple conformations in slow or intermediate exchange with the unfolded state at urea concentrations above 4*M*, concentrations at which the protein has been shown to be unfolded by fluorescence and CD criteria. However, it is obvious that not all aromatic residues exhibit the same types of resonance changes in response to denaturant. The observation that some resonances exhibit more dramatic chemical shifts than others indicates that the corresponding residue side chains experience different solvent exposure, potentially due to stable long-range interactions with other atoms in the molecule for those residues. The residual structure observed previously in IFABP is located in the hydrophobic core region of the protein. The homologous region in BABP contains Phe63, Phe79, Phe94, and Tyr97. Phe47 may be included in this region for BABP, although it is not clear whether the homologous residue in IFABP is included in the initiation site.[10,12,14] Despite homology with the IFABP hydrophobic core region, Phe79 and Phe94 do not appear to participate in an initiating site in the ^{19}F NMR analysis of unfolded BABP, with negligible changes in peak area and chemical shift over the range of urea concentrations from 4 to 8*M*.

If the anomalous chemical shift dependence on denaturant concentration for the resonances assigned to Phe17, Phe47 and Phe63 is due to the presence of a residual structure at high denaturant concentrations, sufficiently high denaturant concentrations should drive the unfolding of this state to completion, causing these slope effects to plateau. Although the experiments were carried out to a maximum of 8*M* urea, far above the midpoint of unfolding, these resonances continued to shift without reaching a plateau at the highest denaturant level. High concentrations of guanidine-HCl (5–6*M*) were used to determine if a stronger denaturant could drive the unfolding equilibrium to completion for fully labeled 4FPhe-BABP. Although instrument performance was severely compromised by the presence of these high salt concentrations, the same resonances showed the same behaviors at high concentrations of guanidine-HCl (similar to Fig. 3), suggesting that the observations are not due to anomalous interactions of those residues with urea. As an alternative means to drive the unfolding equilibrium to completion, additional experiments were carried out with fully labeled 4FPhe-BABP in 8*M* urea at increasing temperature (25–50°C, Supporting Information Fig. 1). At temperatures greater than 30°C, all resonances showed similar dependence of chemical shift on temperature (Supporting Information Fig. 2), suggesting that stronger unfolding conditions can completely unfold the conformation(s) responsible for the anomalous dependence of chemical shift on urea concentration for Phe17, Phe47, and Phe63.

Phe47 and Phe63 may come together earlier in folding than other regions of the protein. The two residues are both at the ends of β-strands and physically close together in the native state but are not close to the same β-turns. The turns between β-strands have been presented as a possible site for folding initiation,[22] but in this case, the two residues are on neighboring loops. This may support a slightly different model for folding based on formation of larger loops, such as that proposed by Berezovsky *et al.*, in which loops of 25–30 amino acids are formed at the initial stages of folding as the ends of the loops come together.[23] The final shape of the molecule is then stabilized by secondary contacts resulting in the formation of helices, sheets, and other loop-to-loop contacts. Although the sequence between Phe47 and Phe63 is somewhat shorter than that proposed in this model, the model provides an interesting perspective on how folding could be initiated in BABP. β-strands C and D could be considered to be independent units with the ends interacting at the earliest stage of folding. The stage would then be set for the other hydrophobic residues in the core of the protein to become organized in their correct native contacts and the remaining secondary structure to form rapidly. The two β-strands between Phe47 and Phe63 are analogous to two segments of IFABP that have a strong intrinsic bias in their sequence to form β-strands.[24,25] The perspective that protein folding is similar to folding a carpenter's rule presented by Srinivasan[24] may apply to BABP, with β-strands C and D coming together similar to the way that two hinges in a rule are bent to contact each other without being dependent on the region in between.

There is also the possibility that the two turns that contain Phe63 and Phe47 form independently early in the folding pathway. The chemical shift behavior of the two residues, though greater than that of most other residues observed, is not exactly the same. It could be the case that the two hairpin turns form independently of each other, consistent with the hypothesis of turn formation in folding initiation,[22] and with the observation by Li[14] that IFABP-Phe47 folds independently of IFABP-Phe62. Mutations that disrupt the hydrophobic core of IFABP in the regions of residues 63–66 affect the folding and stabilization of the protein,[26,27] and IFABP-Leu64 has been shown to retain residual structure at high denaturant concentrations.[26,28] The turn between strands D and E, near Phe63, is highly conserved in the iLBP family.[29] This high degree of conservation may indicate an important

role for this turn region in folding initiation for the family, which is supported by the data here.

Earlier kinetic analysis of rat BABP folding had indicated that the protein folds via a simple, reversible mechanism and encounters an on-path intermediate that retains most if not all of its secondary structure.[2] In a more recent study using improved instrumentation, a second intermediate with no remaining secondary structure was observed in the unfolding pathway by stopped-flow fluorescence.[4] This intermediate appears to have some tertiary contacts to other residues and no secondary structure. As this intermediate occurs early in the folding pathway, Phe17, Phe47, and/or Phe63 may be involved in formation of this type of intermediate state. There may be a relationship between an early intermediate observed in IFABP by ^{19}F NMR and the structure observed here in the Phe63/Phe47 region of BABP.

The current data indicate that early contacts in BABP may occur in the hydrophobic core region in a fashion similar to that in IFABP, but the aromatic residues in this core have different ^{19}F NMR characteristics for the two proteins. The evidence supports the presence of an early intermediate conformation in IFABP in exchange with the unfolded state on an intermediate time scale,[12] but no such intermediate has been observed for BABP. However, the data presented here argues that some population of intermediate conformations persists at high denaturant concentration, despite the fact that the protein appears to be unfolded by optical methods. The fact that two of the Phe residues suggested to be involved in this residual structure also lie in the hydrophobic core region of the protein may indicate that hydrophobic collapse may serve as a conserved mechanism for the initiation of folding in the iLBP family.

Materials and Methods

Protein source and expression

All studies used recombinant proteins expressed and purified from *E. coli*. The human BABP proteins and mutants were modified at the N-terminal end with a histidine tag for ease of purification. Purification and expression of all protein mutants was done using the same plasmid; however, the bacterial strains used for protein production varied depending on the type of fluorine labeling. The wild-type strain, BL21(DE3), was used for unlabeled protein, the phenylalanine- and tyrosine-auxotrophic strain DL39(DE3) for uniform labeling of phenylalanine or tyrosine residues, and the K10F6Δ(DE3) strain,[13] for the single-site 4FPhe-labeled proteins.

The plasmid pRO.hBABP (6His) was constructed using the plasmid pRO.148, obtained from Dr. Carl Frieden at Washington University School of Medicine, St. Louis, MO.[30] This plasmid contains the yeast phenylalanine synthetase gene (PheRS) engineered into the PvuII restriction site of pQE.16 (Qiagen), as well as the mouse dihydrofolate reductase (DHFR) gene. The BABP gene was obtained from Dr. D. Cistola at Washington University School of Medicine, St. Louis, MO, and subcloned in our laboratory into the pET28b(+) vector (Novagen) for introduction of a histidine tag at the N-terminus. The histidine-tagged BABP was subcloned into the pRO.148 vector in place of the DHFR gene, and the vector renamed pRO.hBABP(6His).

The methods for incorporation of ^{19}F-amino acid analogs have been described in detail.[30] For a subset of our experiments, analog was incorporated uniformly at all BABP phenylalanine sites, as described for IFABP (Ropson 2006), using DL39(DE3) as the expression vector and inducing protein production with IPTG. For single-site fluorine incorporation, pRO.hBABP (6His) described above was used. The bacterial strain K10F6Δ(DE3) is not auxotrophic for phenylalanine but instead resistant to incorporation of the 4-fluorophenylalanine analog. The system is based on the work of Furter,[13] and utilizes a "21st amino acid codon" method for incorporation of the fluorine analog wherein an amber stop codon is engineered into the gene in place of the selected Phe. K10F6Δ(DE3) cells were cotransformed with the pRO.hBABP(6His) plasmid and the pRO.117 plasmid, which was also obtained from Dr. Frieden's laboratory. The pRO.117 plasmid contains the yeast amber-suppressor $tRNA^{Phe}$, which charges the amber codon as 4FPhe. The only single-site labeled protein that did not express well under these conditions was the plasmid encoding the suppressor tRNA for Phe6. Freshly transformed cells were cultured as described.[30]

Recombinant proteins were purified under denaturing conditions in one step by taking advantage of the six histidine residues engineered onto the N-terminus of BABP. The protocol was modified from that recommended by the manufacturer for use with the His-SELECT Ni-NTA resin (Sigma). Cell pellets were stored at −80° before purification, and cells disrupted by the freeze-thaw method[31] in the presence of 8*M* urea in standard buffer (10 m*M* Na_2HPO_4, 15 m*M* NaH_2PO_4, 75 m*M* NaCl, 0.1 m*M* EDTA, pH 8.0). After three rounds of centrifugation and washing of the freeze-thawed cells with urea containing buffer, the combined supernatants contained denatured protein. The Ni-NTA column was equilibrated with the same 8*M* urea buffer, and the combined supernatants loaded onto the column, then washed with 8*M* urea buffer until the OD_{280} of the eluate had stabilized. A gradient mixer was used to apply a linear gradient of 8–0*M* urea in buffer totaling five column volumes. The column was then rinsed with three column volumes of wash buffer (50 m*M* NaH_2PO_4, 100 m*M* NaCl, 2 m*M* imidazole, pH = 8.0) to ensure complete removal of all denaturant. Nonspecific protein contaminants were removed

from the resin with two column volumes of wash buffer containing 10 m*M* imidazole followed by two column volumes containing 25 m*M* imidazole. The histidine-tagged protein was eluted with buffer containing 100 m*M* imidazole until the OD_{280} fell to baseline values, and a final wash with 250 m*M* imidazole to ensure complete removal of all protein. Aliquots of the fractions collected from the column were run on a 4–20% gradient SDS-PAGE gel to determine the fractions containing protein. Fractions showing a single band of appropriate molecular weight were combined, concentrated by Amicon Ultrafiltration, and used without further purification. The product was dialyzed against NMR buffer for complete removal of imidazole and buffer exchange, and the final product lyophilized for use in the NMR experiments.

Protein concentrations were determined by optical density at 280 nm, with the molar absorption coefficient estimated to be 11,460 M^{-1} cm^{-1} using the calculation described by Pace.[32] All chemicals used were of reagent grade. 4FPhe, 3FTyr, and 6FTrp were obtained from Sigma. Stocks of 4FPhe (30 m*M*) were prepared, sterile-filtered through a 0.22 μ*M* nylon membrane, and stored at 4° until use. Ultra pure grade urea was obtained from Amresco (Solon, Ohio); stocks of 10*M* urea were prepared ahead of time and stored at −20°.[33] Urea concentrations were determined by refractive index at 25° using a Milton-Roy Abbe-3 refractometer as previously described.[34]

Fluorometry

Fluorescence measurements of unfolding were done by preparing stock solutions of 0.1 mg/mL protein in either 9*M* urea or standard buffer, both at pH 8.0. Samples for a range of urea concentrations were prepared by dilution of the stock solutions into each other using a Hamilton titrator. All samples were equilibrated at 25° for a minimum of 1 h before use. Samples (300 μL) were transferred to a 3-mm square cuvette, placed in the PTI Alphascan spectrofluorometer equilibrated at 25° and incubated for at least 2 min to ensure temperature equilibration before data collection. The excitation wavelength was set at 290 nm with a 5 nm band pass and the emission collected over the range of 305–400 nm with a 6 nm band pass. Fits are shown to the emission intensity at 360 nm (Fig. 2), although other wavelengths were recorded and analyzed to confirm the results. Data were fit to a two-state model by nonlinear least-squares methods using KaleidaGraph (Synergy Software) as described.[3,35]

NMR

Samples for ^{19}F NMR were prepared by dialysis of the purified protein against dilute NMR buffer, pH 8.0. To analyze 5-mg total protein per run in a 0.6-mL final volume, 8.3 mg of protein was dialyzed against an appropriately diluted buffer such that resuspension to 1 mL would yield a 1x buffer concentration. For example, 10 mL of a protein solution at 0.83 mg/mL was dialyzed against 1/10x buffer (standard NMR buffer: 25 m*M* PO_4, 75 m*M* NaCl, 0.1 m*M* EDTA, pH 8.0), such that resuspension in 1 mL water resulted in 8.3 mg protein in 1x NMR buffer. Two 8.3 mg aliquots of each labeled protein were prepared, lyophilized, and stored at –20° until use. On the day of data collection, the stocks were resuspended in either 1-mL H_2O (10% D_2O) or 1-mL 8*M* urea (10% D_2O). After data collection at 0 and 8*M* urea, samples were recovered and manually mixed to obtain the desired urea concentrations. Samples were equilibrated in the spectrometer for at least 5 min at 25° before data collection. NMR data were collected as described for IFABP.[6] A Bruker Avance 500 digital NMR spectrometer was used in conjunction with a $^{19}F/^{1}H$ dual channel probe for ^{19}F detection with ^{1}H decoupling. Sweep width was set at 35 ppm, and at least 256 transients were collected for each sample. Delay times of 2.5 s and acquisition time of 1 s were chosen to ensure accurate integration based on separate experiments to determine T_1 and T_2 relaxation times of native and unfolded proteins. 6FTrp was used as the reference standard in all experiments, and all reported chemical shifts were in ppm from this reference. Data analysis was performed using the MacNUTS NMR Software package from Acorn NMR. Relative integrated peak intensities were calculated based on a standard concentration of 0.25 m*M* 6FTrp for each sample.

Acknowledgments

The Pennsylvania Department of Health specifically disclaims responsibility for any analyses, interpretations, or conclusions.

References

1. Banaszak L, Winter N, Xu Z, Bernlohr DA, Cowan S, Jones TA (1994) Lipid-binding proteins: a family of fatty acid and retinoid transport proteins. Adv Prot Chem 45: 89–151.
2. Dalessio PM, Ropson IJ (2000) Beta-sheet proteins with nearly identical structures have different folding intermediates. Biochemistry 39:860–871.
3. Burns LL, Dalessio PM, Ropson IJ (1998) Folding mechanism of three structurally similar beta-sheet proteins. Proteins 33:107–118.
4. Dalessio PM, Boyer JA, McGettigan JL, Ropson IJ (2005) Swapping core residues in homologous proteins swaps folding mechanism. Biochemistry 44:3082–3090.
5. Gunasekaran K, Hagler AT, Gierasch LM (2004) Sequence and structural analysis of cellular retinoic acid-binding proteins reveals a network of conserved hydrophobic interactions. Proteins 54:179–194.
6. Ropson IJ, Boyer JA, Schaeffer BA, Dalessio PM (2009) Comparison of the folding mechanism of highly homologous proteins in the lipid-binding protein family. Proteins 75:799–806.
7. Ropson IJ, Frieden C (1992) Dynamic NMR spectral analysis and protein folding: identification of a highly

populated folding intermediate of rat intestinal fatty acid-binding protein by ^{19}F-NMR. Proc Natl Acad Sci USA 89:7222–7226.
8. Yeh S-R, Ropson IJ, Rousseau DL (2001) Hierarchical folding of intestinal fatty acid binding protein. Biochemistry 40:4205–4210.
9. Dalessio PM, Fromholt SE, Ropson IJ (2005) The role of Trp-82 in the folding of intestinal fatty acid binding protein. Proteins 61:176–183.
10. Li H, Frieden C (2005) Phenylalanine side chain behavior of the intestinal fatty acid binding protein: the effect of urea on backbone and side chain stability. JBC 280:38556–38561.
11. Li H, Frieden C (2007) Observation of sequential steps in the folding of intestinal fatty acid binding protein using a slow folding mutant and ^{19}F NMR. Proc Natl Acad Sci USA 104:11993–11998.
12. Ropson IJ, Boyer JA, Dalessio PM (2006) A residual structure in unfolded intestinal fatty acid binding protein consists of amino acids that are neighbors in the native state Biochemistry 45:2608–2617.
13. Furter R (1998) Expansion of the genetic code: site-directed p-fluoro-phenylalanine incorporation in *Escherichia coli*. Protein Sci 7:419–426.
14. Li H, Frieden C (2005) NMR Studies of 4-19F-Phenylalanine-labeled intestinal fatty acid-binding protein: evidence for conformational heterogeneity in the native state. Biochemistry 44:2369–2377.
15. Ogbay B, Dekoster GT, Cistola DP (2003) The NMR structure of a stable and compact all-beta-sheet variant of intestinal fatty acid-binding protein. Protein Sci 13:1227–1237.
16. Kim K, Cistola DP, Frieden CF (1996) Intestinal fatty acid-binding protein: the structure and stability of a helix-less variant. Biochemistry 35:7553–7558.
17. Kouvatsos N, Meldrum JK, Searle MS, Thomas NR (2006) Coupling of ligand recognition to protein folding in an engineered variant of rabbit ileal lipid binding protein. Chem Commun (Camb) 44:4623–4625.
18. Sukumar M, Gierasch LM (1997) Local interactions in a Schellman motif dictate interhelical arrangement in a protein fragment. Fold Des 2:211–222.
19. Lacroix E, Viguera AR, Serrano L (1998) Elucidating the folding problem of alpha-helices: Local motifs, long-range electrostatics, ionic strength dependence and prediction of NMR parameters. J Mol Biol 284:173–191.
20. Gerig JT (2001) Fluorine NMR. Online textbook <http://www.biophysics.org/Portals/1/PDFs/Education/gerig.pdf>. Accessed on January 4, 2011.
21. Danielson MA, Falke JJ (1996) Use of 19F-NMR to probe protein structure and conformation changes. Annu Rev Biophys Biomol Struct 25:163–195.
22. Muñoz V, Henry ER, Hofrichter J, Eaton WA (1998) A statistical mechanical model for beta-hairpin kinetics. Proc Natl Acad Sci USA 95:5872–5879.
23. Berezovsky IN, Kirzhner VM, Kirzhner A, Trifonov EN (2001) Protein folding: looping from hydrophobic nuclei. Proteins 45:346–350.
24. Srinivasan R, Rose GD (1999) A physical basis for protein secondary structure. Proc Natl Acad Sci USA 96: 14258–14263.
25. Nikiforovich GV, Frieden C (2002) The search for local native-like nucleation centers in the unfolded state of beta-sheet proteins. Proc Natl Acad Sci USA 99:10388–10393.
26. Kim K, Ramanathan R, Frieden C (1997) Intestinal fatty acid binding protein: a specific residue in one turn appears to stabilize the native structure and be responsible for slow folding. Protein Sci 6:364–372.
27. Rajabzadeh M, Kao J, Frieden C (2003) Consequences of single-site mutations in the intestinal fatty acid binding protein. Biochemistry 42:12192–12199.
28. Hodsdon ME, Frieden C (2001) Intestinal fatty acid binding protein: the folding mechanism as determined by NMR studies. Biochemistry 40:732–742.
29. Rotondi KS, Gierasch LM (2003) Role of local sequence in the folding of cellular retinoic acid binding protein. I. structural propensities of reverse turns. Biochemistry 42:7976–7985.
30. Frieden C, Hoeltzli SD, Bann JG (2004) The preparation of 19F-labeled proteins for NMR studies. Methods Enzymol 380:400–415.
31. Johnson BH, Hecht MH (1994) Recombinant proteins can be isolated from *E. coli* cells by repeated cycles of freezing and thawing. Biotechnology 12:1357–1360.
32. Pace CN, Vajdos F, Fee L, Grimsley G, Gray T (1995) How to measure and predict the molar absorption coefficient of a protein. Protein Sci 4:2411–2423.
33. Ropson IJ, Dalessio PM (1997) Fluorescence spectral changes during the folding of intestinal fatty acid binding protein. Biochemistry 36:8594–8601.
34. Pace CN (1986) Determination and analysis of urea and guanidine HCl denaturation curves. Meth Enzymol 131:266–281
35. Bolen DW, Santoro MM (1988) Unfolding free energy changes determined by the linear extrapolation method. 2. Incorporation of delta G degrees N-U values in a thermodynamic cycle. Biochemistry 27:8069–8074.